Atmos. Meas. Tech. Discuss., 5, 5993–6035, 2012
www.atmos-meas-tech-discuss.net/5/5993/2012/
doi:10.5194/amtd-5-5993-2012

Atmospheric Measurement Techniques Discussions

Global stratospheric aerosol extinction profile retrievals from SCIAMACHY limb-scatter observations

F. Ernst[1], C. von Savigny[1,*], A. Rozanov[1], V. Rozanov[1], K.-U. Eichmann[1], L. A. Brinkhoff[1], H. Bovensmann[1], and J. P. Burrows[1]

[1]Institute of Environmental Physics/Remote Sensing, University of Bremen, Bremen, Germany
[*]now at: Institute of Physics, Ernst-Moritz-Arndt-University of Greifswald, Greifswald, Germany

Received: 27 July 2012 – Accepted: 7 August 2012 – Published: 21 August 2012

Correspondence to: F. Ernst (fernst@iup.physik.uni-bremen.de)

Published by Copernicus Publications on behalf of the European Geosciences Union.

Abstract

Stratospheric aerosol extinction profiles are retrieved from SCIAMACHY/Envisat limb-scatter observations in the visible spectral range. The retrieval algorithm is based on a colour-index approach using the normalized limb-radiance profiles at 470 nm and 750 nm wavelength. The optimal estimation approach in combination with the radiative transfer model SCIATRAN is employed for the retrievals. This study presents a detailed description of the retrieval algorithm, and a sensitivity analysis investigating the impact of the most important parameters that affect the aerosol extinction profile retrieval accuracy. It is found that the parameter with the largest impact is surface albedo, particularly for SCIAMACHY observations in the Southern Hemisphere where the error in stratospheric aerosol extinction can be up to 50 % if the surface albedo is not well known. The effect of errors in the assumed ozone and neutral density profiles on the aerosol profile retrievals is with generally less than 6 % relatively small. The aerosol extinction profiles retrieved from SCIAMACHY are compared with co-located SAGE II solar occultation measurements of stratospheric aerosol extinction during the period 2003–2005. The mean aerosol extinction profiles averaged over all co-locations agree to within 20 % between 15 and 35 km altitude. However, larger differences are observed at specific latitudes.

1 Introduction

Stratospheric aerosols are of great importance to both the atmosphere's radiative balance and stratospheric chemistry. They scatter solar radiation efficiently and therefore cool the planet by increasing its albedo. Particularly after strong volcanic eruptions the impact of aerosols is significant. For example, after the 1991 eruption of the Philippine volcano Mt. Pinatubo the global mean surface temperature decreased by 1 K over a period of several months (e.g. Self et al., 1997, and references therein). Inside the polar vortex, sulphuric acid aerosols act as condensation nuclei in the formation of

AMTD
5, 5993–6035, 2012

polar stratospheric clouds and participate in the halogen activation facilitating the heterogeneous chemistry that leads to the formation of the ozone hole in Antarctic spring, and to partly significant chemical ozone losses in the Northern Hemisphere lower polar stratosphere during Arctic spring. Outside the polar vortices stratospheric aerosols can also lead to chlorine activation (Erle et al., 1998; Hanson and Ravishankara, 1995; Solomon et al., 1993).

Stratospheric aerosol is composed primarily of sulfuric acid (75 %) and water (25 %) during both volcanically active and quiescent periods (Junge et al., 1961; Rosen, 1971). The background aerosol particles have radii on the order of 0.1–0.5 µm with a concentration of 0.005–0.5 cm^{-3} (Deshler, 2008). The source for these non-volcanic particles is injection of tropospheric air containing OCS, SO_2, and sulfate particles by tropical convection. The source gases are photo-dissociated and oxidized, followed by nucleation and condensation in the tropics leading to accumulation of sulfuric acid droplets. These are transported pole-ward and downward in the global planetary wave driven tropical pump, leading to a quasi steady state maximum in particle number density at around 20 km in the mid latitudes. After large volcanic eruptions the particle radius increases by a factor of 2–4, and concentration by a factor of 10–1000 (Deshler, 2008).

Global and continuous observations of stratospheric aerosols are essential for monitoring the spatial distribution of volcanic aerosols with time as well as the long-term variation of stratospheric aerosols in general. These observations can only be provided by satellite measurements. The observation technique traditionally used to measure stratospheric aerosol extinction profiles is solar occultation. It has been used, e.g. by the SAM (Stratospheric Aerosol Measurement) (e.g. McCormick and Trepte, 1986), the SAGE (Stratospheric Aerosol and Gas Experiment) (e.g. McCormick and Veiga, 1992), and POAM (Polar Ozone and Aerosol Measurement) (e.g. Lumpe et al., 1997) instrument series. Solar occultation observations provide accurate aerosol extinction profiles typically with high vertical resolution at multiple wavelengths, and the spectral dependence of the extinction coefficients allows inferring information on the aerosol particle size (Lenoble et al., 1984; Brogniez et al., 1992; Brogniez and Lenoble, 1988).

The disadvantage of solar occultation measurements is that the number of occultations is limited to one sunrise and one sunset observation per orbit at most. Moreover, the latitudes of these observations change only slowly with time. Stellar occultation, e.g. by GOMOS (Global Ozone Monitoring by Occultation of Stars) (Bertaux et al., 1991) can also be used to measure multi-spectral aerosol extinction profiles providing significantly enhanced geographical coverage.

A new generation of instruments employ limb observations of the scattered solar radiation to retrieve vertical profiles of trace constituents and stratospheric aerosols. This technique combines high vertical resolution with near-global coverage, but requires sophisticated radiative transfer modelling to perform the retrieval.

Before the year 2000 only very few studies – and only carried out with non-orbiting instruments – employed limb-radiance measurements to infer stratospheric aerosol extinction coefficients or size parameters. Cunnold et al. (1973) used photometer measurements of limb-scattered sunlight made from the X-15 aircraft at 6 spectral intervals to infer aerosol extinction profiles with an optimal estimation scheme. Ackermann et al. (1981) used balloon-borne photographic observations of the azimuthal variation of limb-radiances to establish the aerosol phase function. McLinden et al. (1999) employed profiles of limb-radiance and the degree of linear polarization measured with the CPFM instrument flown aboard NASA's ER-2 plane to retrieve vertical profiles of stratospheric aerosol number density and size parameters.

SCIAMACHY, the Scanning Imaging Absorption SpectroMeter for Atmospheric CHartography (Burrows et al., 1995; Bovensmann et al., 1999, and references therein) on ESA's Envisat spacecraft is one such instrument employing the limb-scatter observation geometry. Others include the Optical Spectrograph and Infrared Imaging System (OSIRIS) on the Swedish/Canadian/Finnish/French Odin satellite (Llewellyn et al., 2004). Furthermore, the recently launched Ozone Mapping/Profiler Suite (OMPS) aboard NPP (NPOESS preparatory mission, where NPOESS stands for National Polar-orbiting Operational Environmental Satellite) also performs limb-scatter observations (Lee et al., 2010).

AMTD
5, 5993–6035, 2012

Title Page
Abstract | Introduction
Conclusions | References
Tables | Figures
◀| |▶
◀ ▶
Back | Close
Full Screen / Esc
Printer-friendly Version
Interactive Discussion

In this study we employ limb-scatter measurements with the SCIAMACHY instrument to retrieve stratospheric aerosol extinction profiles. Stratospheric aerosols were recently also retrieved from SCIAMACHY limb observations by Taha et al. (2011) and Ovigneur et al. (2011), but with different retrieval methods. Taha et al. (2011) applied the retrieval algorithm developed for the analysis of OMPS limb profiler observations to a limited SCIAMACHY data set. In contrast to the retrieval scheme applied in this study Taha et al. (2011) retrieved aerosol extinction profiles from limb radiance profile measurements at individual wavelengths. Ovigneur et al. (2011) used SCIAMACHY limb-radiance measurements in the O_2 A-band region to retrieve stratospheric aerosol number densities. The retrieval scheme exploits the light path difference within and outside the O_2 A-band to retrieve stratospheric aerosol information.

The paper is structured as follows. Section 2 provides a brief description of the SCIAMACHY instrument. The retrieval algorithm is described in detail in the following Sect. 3. The sensitivity studies carried out in order to establish an error budget of the stratospheric aerosol extinction retrievals are presented in Sect. 4, and Sect. 5 provides comparisons between SAGE II and SCIAMACHY stratospheric aerosol extinction profiles. First results on the global stratospheric aerosol morphology retrieved from SCIAMACHY limb scatter observations and for the years 2003–2010 are shown and discussed in Sect. 6. Conclusions are presented at the end.

2 SCIAMACHY on Envisat

The SCanning Imaging Absorption spectroMeter for Atmospheric CHartographY (SCIAMACHY) (Burrows et al., 1995; Bovensmann et al., 1999) was launched as one of ten instruments on board the European environmental research satellite Envisat on 1 March 2002. Envisat was injected into a polar, sun-synchronous orbit with a descending node equator crossing time of 10:00 LT. The Envisat mission abruptly ended in April 2012 as a consequence of a major spacecraft failure of currently unknown origin. SCIAMACHY measured solar radiation, which was transmitted through or scattered by the atmosphere in nadir, limb-scatter and occultation mode. This study uses limb-scatter observations. SCIAMACHY was a double monochromator comprising a dispersing prism and grating spectrometers observing the 220–2380 nm spectral range in 8 spectral channels. With a geometrical field of view of 2.6 km in vertical direction and 110 km in horizontal direction, it scanned the atmosphere from 0 to 92 km in tangent height steps of 3.3 km in the nominal limb-scatter mode (Gottwald and Bovensmann, 2011). The retrievals performed as part of this study are based on SCIAMACHY Level 1 data version 7.03. The Level 1 data were calibrated with all options but flags 0, 6, and 7, i.e. memory effect correction, polarization correction and absolute calibration were not performed, as a result of remaining issues with these calibration steps.

3 Algorithm description

Stratospheric aerosol extinction profiles are retrieved from SCIAMACHY observations of limb-radiance profiles at two wavelengths using a color-index approach. The two wavelengths are $\lambda_s = 470$ nm and $\lambda_l = 750$ nm (where s/l stands for short/long wavelength). Spectral windows with weak atmospheric absorption are preferred in order to avoid retrieval errors caused by incorrect knowledge of absorber profiles. Both wavelengths used are sufficiently distant from the center of the Chappuis absorption band of O_3 near 600 nm. λ_s falls between an NO_2 and the Chappuis absorption band, and λ_l is just below the O_2 A-band. The measurement vector required for the retrieval is derived from the limb-radiance profiles at the two wavelengths using a 2-step approach, following the method previously used by Bourassa et al. (2007).

First we normalize the limb-radiance at each tangent height with the radiance at a reference tangent height of the same limb-radiance profile:

$$I_N^\lambda(\mathrm{TH}) = \frac{I^\lambda(\mathrm{TH})}{I^\lambda(\mathrm{TH_{ref}})} \tag{1}$$

where subscript N indicates normalization.

AMTD
5, 5993–6035, 2012
Stratospheric aerosol profiles from SCIAMACHY
F. Ernst et al.

This technique is adapted from trace gas retrievals (e.g. Flittner et al., 2000; von Savigny et al., 2003) and adjusted for the aerosol retrieval. It has two advantages: first, an absolute calibration of the limb-radiances is not required. Furthermore, von Savigny et al. (2003) showed that the tangent height normalization leads to a reduced sensitivity to errors in the assumed ground albedo. This is based on the assumption that the fraction of ground-reflected sunlight in the limb-radiance is similar at all tangent heights, including the reference tangent height. A reference tangent height (TH_{ref}) of 35 km was chosen because at this point (and above) the aerosol loading in the atmosphere is small under background conditions. Above that tangent height the SCIAMACHY limb measurements are potentially contaminated by external or "baffle" straylight.

Figure 1 illustrates the effect of the tangent height normalization on limb-radiance profiles for a polar and a tropical scenario using simulated radiance profiles for λ_s = 470 nm (blue) and λ_l = 750 nm (red) with 7 different ground albedos. For the two latitudes 83° N and 0°, respectively, typical SCIAMACHY geometries have been simulated, with solar zenith angles at tangent point (SZA@TP) of 84° and 36°, respectively, and solar azimuth angles at tangent point (SAA@TP) of 38° and 105°, respectively (see Table 1). The modified ECSTRA (Extinction Coefficient for STRatospheric Aerosol, Fussen and Bingen, 1999) profiles for the two latitudes have been used as aerosol extinction profile (see Sect. 3.4).

The unnormalized radiance profiles for the two latitudes (Fig. 1a, c) show a much larger impact of the ground albedo at the equator (note the factor of ten between the two abscissas of the difference plots). The reason for this is the smaller solar zenith angle in the tropics, which leads to a larger fraction of radiation reaching the earth's surface, being reflected from the surface and finally scattered into the field of view of the instrument. The tangent height normalization (Fig. 1b, d) leads to a significant decrease of the albedo influence by roughly a factor of 10 at both latitudes. Interestingly, the sign of the difference changes for the polar geometry while it stays the same for the tropical geometry.

AMTD
5, 5993–6035, 2012

In a second step we combine the normalized limb-radiance profiles at the two wavelengths in a color-index-ratio. Retrieving aerosol extinction profiles from limb-radiance profiles at a single wavelength is also an option, but it relies on the assumption that the background Rayleigh atmosphere can be modelled perfectly. Any uncertainty in the neutral density would result in an error in the aerosol profile. To reduce this effect, it is suitable to use the ratio of a long to a short wavelength. Since the Ångstrøm exponent for Mie-scattering is highly variable – but for stratospheric aerosols generally significantly smaller than for Rayleigh scattering ($\alpha \approx 4$) – wavelength pairing provides a suitable measurement vector for the retrieval of stratospheric aerosols. Instead of the simple ratio of the two normalized limb-radiance profiles, we use the natural logarithm of the ratio as the retrieval vector for the inversion (see below). The wavelength pairing can then be described mathematically as follows:

$$\boldsymbol{y}(\mathrm{TH}) = \ln\left(\frac{I_N^{\lambda_l}(\mathrm{TH})}{I_N^{\lambda_s}(\mathrm{TH})}\right) \tag{2}$$

where $\boldsymbol{y}$ is the measurement vector.

Figure 2 shows the effect of the wavelength pairing for the two geometries used above. On the left side the tangent height normalized radiances of the two wavelengths are plotted separately with and without aerosol loading. The right side shows the logarithms of the color-index-ratio as described above. The difference between the aerosol case and the no-aerosol case is increased significantly.

Obtaining stratospheric aerosol extinction coefficient profiles from SCIAMACHY limb-radiance profiles is an inverse problem, requiring the inversion of the following generic equation:

$$\boldsymbol{y} = \mathbf{K}\boldsymbol{x} + \epsilon, \tag{3}$$

where $\boldsymbol{y}$ is the so-called measurement vector. In our case the measurement vector contains logarithms of the normalized and paired limb-radiance profiles at each selected tangent height – as described above. $\boldsymbol{x}$ is the so-called state vector, representing the height distribution of the desired atmospheric parameter, i.e. in this case the aerosol extinction coefficient at each altitude. $\mathbf{K}$ is the weighting function matrix or Jacobian matrix. ϵ contains all errors. The main task of this work is to retrieve the aerosol extinction coefficient profile $\boldsymbol{x}$ from the SCIAMACHY normalized and paired radiance profile $\boldsymbol{y}$. In order to solve the inversion problem we employ the optimal estimation technique – briefly described in the following Sect. 3.1 – in combination with the radiative transfer model SCIATRAN – described in Sect. 3.2.

3.1 Optimal estimation method

In SCIATRAN, Eq. (3) is used in form of

$$\hat{\boldsymbol{y}} = \hat{\boldsymbol{x}} + \epsilon, \tag{4}$$

where $\hat{\boldsymbol{y}} = \boldsymbol{y} - \boldsymbol{y}_0$ is the measurement vector containing the differences between logarithms of measured and simulated spectra (both normalized and paired) and $\hat{\boldsymbol{x}} = (\boldsymbol{x} - \boldsymbol{x}_0)/\boldsymbol{x}_0$ is the state vector containing relative differences between the a priori and retrieved aerosol extinction profiles. Following Rodgers (2000), the solution of Eq. (4) is found as

$$\boldsymbol{x} = \boldsymbol{x}_0 + (\mathbf{K}^{\mathrm{T}}\mathbf{S}_y^{-1}\mathbf{K} + \mathbf{S}_{\mathrm{a}}^{-1})^{-1}\mathbf{K}^{\mathrm{T}}\mathbf{S}_y^{-1}(\boldsymbol{y} - \boldsymbol{y}_0)\boldsymbol{x}_0 \tag{5}$$

with $\mathbf{S}_{\mathrm{a}}$ as the a priori covariance matrix and $\mathbf{S}_y$ as the noise covariance matrix. Because of the non-linearity of the problem, the forward model and retrieval code SCIATRAN version 3.1 (Rozanov et al., 2005) is used to find the solution iteratively:

$$\boldsymbol{x}_{i+1} = \boldsymbol{x}_0 + (\mathbf{K}_i^{\mathrm{T}}\mathbf{S}_y^{-1}\mathbf{K}_i + \mathbf{S}_{\mathrm{a}}^{-1})^{-1}\mathbf{K}_i^{\mathrm{T}}\mathbf{S}_y^{-1}(\boldsymbol{y} - \boldsymbol{y}_i + \mathbf{K}_i(\boldsymbol{x}_i - \boldsymbol{x}_0)/\boldsymbol{x}_0)\boldsymbol{x}_0 \tag{6}$$

with $\mathbf{S}_i = (\mathbf{K}_i^{\mathrm{T}}\mathbf{S}_y^{-1}\mathbf{K}_i + \mathbf{S}_{\mathrm{a}}^{-1})^{-1}$ as the solution covariance matrix.

The noise covariance matrix is chosen to be diagonal, i.e. the errors are assumed to be uncorrelated. The N/S value of 0.005 is used for all tangent heights and spectral

AMTD
5, 5993–6035, 2012

points. In terms of the a priori covariance matrix the non-diagonal elements drop off exponentially with a correlation radius of 3.3 km and the diagonal elements correspond to a relative standard deviation of 1.

3.2 SCIATRAN model

SCIATRAN is a linearized radiative transfer model designed to simulate the scattered solar radiation and the weighting functions of various atmospheric parameters in the UV-Visible-near-IR spectral range for any viewing geometry (nadir, zenith, off-axis, limb, etc.) and any observer position within and outside the atmosphere. The software package also contains a retrieval algorithm, which can be easily adjusted to solve a wide range of scientific tasks. For this work, version 3.1 (Rozanov et al., 2005) was extended for the retrieval of aerosols. SCIATRAN allows for a field of view integration to take the finite vertical resolution of the SCIAMACHY limb-measurements into account. The retrieval altitude grid is a regular 1 km grid.

3.3 Aerosol parameterization in SCIATRAN

For this retrieval, SCIATRAN uses the Henyey-Greenstein approximation for the aerosol phase function (Henyey and Greenstein, 1941). Equation (7) describes the phase function at scattering angle a and for asymmetry parameter g.

$$\Phi(a) = \frac{1}{4\pi} \frac{(1-g^2)}{(1+g^2-2g\cos a)^{3/2}} \tag{7}$$

The extinction and scattering coefficients of 4 water soluble and 8 insoluble aerosol components are calculated by a standard Mie programm (Kauss, 1998; Hoogen, 1995; Wiscombe, 1980), in this case for sulfate aerosols at 0 % relative humidity. The second expansion coefficient of the Legendre series is used as wavelength-dependent asymmetry parameter for the Henyey-Greenstein approximation. Figure 3 shows the Henyey-Greenstein phase functions for 470 and 750 nm.

AMTD
5, 5993–6035, 2012

The size distribution of the stratospheric sulfate aerosols is assumed to be lognormal (Davies, 1974) with a mode radius of 0.1 µm for a relative humidity of 0 % (Kauss, 1998).

3.4 A priori aerosol extinction profiles

The a priori aerosol extinction profiles required for the retrievals were determined with the ECSTRA model by Fussen and Bingen (1999). ECSTRA is a climatological model of vertical extinction coefficient profiles of stratospheric aerosols in the UV-visible range as a function of wavelength, month, latitude, and volcanism level represented by the aerosol optical depth. The ECSTRA model is based on SAGE II stratospheric aerosol extinction profile data. ECSTRA provides aerosol extinction profiles above the tropopause only, and the tropopause height was taken – depending on latitude and month of the year – from the climatological tropopause height data set by Randel et al. (2000). The vertical structure of the ECSTRA aerosol profile climatology describes the tropopause region, the Junge layer and the high altitude domain (Fussen and Bingen, 1999).

For the retrieval sensitivity studies described below (see Sect. 4) we calculated aerosol extinction profiles for 5 different latitudes (83° N, 40° N, 0°, 40° S, and 75° S) and the month of September with a stratospheric aerosol optical depth of 10^{-3} corresponding to a background aerosol loading without preceding volcanic activity (Thomason et al., 2006). The ECSTRA aerosol extinction profiles were extrapolated exponentially above 30 km with a scale height of 4 km, based on Thomason et al. (2006), and we removed the edge below the tropopause that is generated by the ECSTRA model. Figure 4 shows the modified ECSTRA profiles for the five latitudes. It turned out that the modified ECSTRA profile for 75° S worked best as a priori profile for the retrieval of the aerosol extinction profiles at all SCIAMACHY latitudes. This profile has been used to obtain the results presented in Sect. 5.

AMTD
5, 5993–6035, 2012

4 Sensitivity studies

The retrieval of stratospheric aerosol extinction profiles discussed here is based on measurements of limb-scattered solar radiation. Unfortunately, the observed limb-radiances do not only depend on the aerosol extinction profiles, but on several other geophysical parameters (e.g. surface albedo, neutral density, and potentially minor constituent profiles), instrumental effects (e.g. tangent height errors) as well as retrieval parameters, such as the assumed a priori aerosol extinction profile. In order to quantify the effects of these parameters on the retrieval results, sensitivity analyses were performed for the most important effects. The following subsections deal with the effect of the a priori profiles (Sect. 4.1), errors in the assumed surface albedo (Sect. 4.2), neutral density profiles (Sect. 4.3), ozone profiles (Sect. 4.4), and errors in the tangent height registration (Sect. 4.5).

The general approach used for these sensitivity studies is to perform forward model runs with different settings – i.e. introducing artificial errors – for the specific parameter to be investigated, leaving all other settings unchanged. The simulated limb-radiance profiles are then used as input data for a retrieval with the standard parameter set. The effect on the aerosol extinction profile retrievals is quantified in terms of the relative difference between retrieved and the true aerosol profile (retrieved – true)/true.

4.1 Impact of a priori profile

The retrieval algorithm was tested by performing retrievals with synthetic, i.e. forward modelled observations. For these we modified our a priori aerosol extinction profiles in six different ways – as described below – and used these as aerosol extinction profiles for SCIATRAN forward model runs that produce the synthetic observations. The six modifications are multiplication with a factor of 0.5 and 2, a height shift of the complete profile of ±3 km, and an artificial minimum/maximum around an altitude of 25 km. Then we ran the retrieval with the unmodified a priori profile without changing any other parameter to see if the true profiles are reproduced by the retrieval. Figure 5 shows the

AMTD
5, 5993–6035, 2012

results of the synthetic retrievals. The relative error is generally on the order of a few percent and is below 10 % even in the worst case. We conclude that the retrieval works well in a general sense and that it reacts relatively insensitively to a priori profiles that may not well represent the true aerosol extinction profile.

4.2 Effect of surface albedo

Figure 6 shows the relative error in the retrieved aerosol extinction coefficient for different true albedo values with respect to an assumed albedo of 0.5 as a function of the ground albedo and altitude. Five typical SCIAMACHY geometries are simulated here, for latitudes ranging from 83° N to 75° S (see Table 1) for northern fall equinox to allow a comparison of the two hemispheres. The first 3 panels, corresponding to 83° N, 40° N and 0°, show that the sensitivity of the retrieval to the ground albedo is much higher in the tropics (with errors of up to 40 %) than in the northern polar regions (with errors of about 2 %). Due to the smaller solar zenith angle of the SCIAMACHY observations in the tropics, a larger part of the sunlight is reflected by the ground and scattered into the instrument. The tangent height normalization (see Sect. 3) is not capable of fully compensating for this effect. Comparing the two hemispheres – 40° N and 40° S in particular – indicates that the retrieval is far more sensitive to the ground albedo in the Southern Hemisphere. This finding is consistent with the general shape of the aerosol scattering phase function and the latitudinal variation of the scattering angle associated with SCIAMACHY limb-scatter observations, which shows a smooth transition from small scattering angles at high northern latitudes to large scattering angles at high southern latitudes. A typical aerosol phase function has much smaller values at larger scattering angles, corresponding to the larger solar azimuth angles in southern latitudes (see Table 1). In other words: at 40° S, a larger amount of aerosols is needed to compensate for the same albedo error than at 40° N.

We also note that apart from the highest northern latitude studied (83° N) a low bias in the assumed surface albedo will lead to a high bias in the retrieved aerosol extinction values.

Discussion Paper | Discussion Paper | Discussion Paper | Discussion Paper |

AMTD

5, 5993–6035, 2012

Stratospheric aerosol profiles from SCIAMACHY

F. Ernst et al.

4.3 Effect of neutral density

For the same latitudes and viewing angles as above, we investigated the effect of errors in the neutral density profile on the aerosol profile retrievals. The neutral density profile has a direct impact on the limb-radiance profiles, because it determines the Rayleigh scattering contribution to the limb-radiances. In SCIATRAN the neutral density at all altitudes can be adjusted by the ground pressure, using a constant temperature profile. Figure 7 shows the result of changing the ground pressure by ±30 hPa relative to a reference pressure of 1013 hPa, corresponding to a roughly 3 % perturbation in the density at all altitudes. The effect is generally below 10 % at all latitudes for altitudes above 20 km.

4.4 Effect of ozone

To investigate the effect of an error in the assumed ozone profile on the retrieval, we scaled the entire ozone profile by ±15 % for polar and tropical geometry. SCIATRAN allows to scale the ozone profiles – which are taken from the MPI-C (Max Planck Institute for Chemistry) stratospheric ozone climatology using monthly and zonal means at 10 degree latitude bins – with a manually set total column. In the standard runs we chose typical values of total ozone column for the reference case: 400 DU for polar latitudes and 250 DU for tropical latitudes. For the sensitivity study these reference columns were then perturbed by ±15 %. The SCIAMACHY geometry is simulated for the two latitudes. Figure 8 shows the result of the sensitivity study. Even for the polar scenario with a large total ozone abundance, the impact on the aerosol extinction is below 2 %. The main reason why the stratospheric aerosol retrieval is relatively independent of the stratospheric ozone profile is that λ_s = 470 nm and λ_l = 750 nm are well outside the center of the Chappuis absorption bands of ozone, and the ozone absorption cross section is relatively small at these wavelengths.

Discussion Paper | Discussion Paper | Discussion Paper | Discussion Paper |

AMTD

5, 5993–6035, 2012

Stratospheric aerosol profiles from SCIAMACHY

F. Ernst et al.

4.5 Effect of tangent height errors

Another error source for the retrieval of aerosol extinction profiles are errors in the tangent height registration of the SCIAMACHY limb-scatter observations. Older versions of the SCIAMACHY level 1 data set (lower than version 6.0) were affected by TH errors of up to several kilometers (von Savigny et al., 2005). The currently used versions 7.03 and 7.04 are associated with TH errors of a few hundred meters at most. To investigate this effect, we shifted all tangent heights by ±200 m, ±500 m and ±1000 m. Figure 9 shows the impact on the aerosol extinction profiles at 40° N latitude. Above an altitude of about 20 km, this impact is below 20 % for the 1000 m shift, while below the error can be quite large, up to 45 % at 16 km for a tangent height error of 1000 m. For a typical SCIAMACHY tangent height error of ±200 m (von Savigny et al., 2009), the impact on the aerosol extinction has a maximum of about 8 % at 16 km and is smaller than 5 % above 20 km.

4.6 Summary of the sources of potential systematic errors

The Tables 2 and 3 provide an overview of the sensitivity study results described above. Listed in Table 2 are the retrieval errors – at the five different latitudes – associated with uncertainties in the knowledge of surface albedo and the neutral density profile. Table 3 shows the retrieval errors corresponding to uncertainties in the ozone profile for a polar (83° N) and a tropical (0°) viewing geometry, and in tangent height registration at 40° N. The assumed albedo error is 0.15 (with respect to $A = 0.5$), the assumed error in the neutral density profile is 3 % (scaling with altitude independent factor), and the error in the ozone profile is 15 % (scaling with altitude independent factor). The tangent height error is 200 m.

AMTD

5, 5993–6035, 2012

Stratospheric aerosol profiles from SCIAMACHY

F. Ernst et al.

5 Comparison with SAGE II aerosol extinction profiles

In order to test the applicability of the retrieval approach to real SCIAMACHY limb-scatter observations we analyzed the entire SCIAMACHY data set from August 2002–April 2011 with the retrieval scheme described above in Sect. 3. The aerosol extinction is retrieved at the SCIAMACHY tangent height steps 6–13, corresponding to tangent altitudes of approx. 12–35 km. We used the 75° S modified ECSTRA aerosol extinction profile as a priori profile for all latitudes (see Sect. 3.4). To determine the ground albedo, we used the Matthews database (Matthews, 1983) which considers vegetation, land use, and land cover on a 1° × 1° grid. In order to verify the validity of our retrieval approach, we compared the retrieved aerosol extinction profiles with co-located SAGE II measurements. SAGE II (Stratospheric Aerosol and Gas Experiment) (e.g. Thomason, 1991) performed solar occultation observations from 1984 to 2005 and provided as one of the data products stratospheric aerosol extinction profiles at 525 nm wavelength. The SAGE II stratospheric aerosol data set is generally considered to be one of the stratospheric aerosol data sets with the highest accuracy, and is therefore well suited to serve as a benchmark for comparisons with the SCIAMACHY results presented here. For comparison we used all SCIAMACHY limb observations between 1 January 2003 and 17 August 2005 within a spatial distance of 500 km and a temporal difference of 6 h at most to a SAGE II measurement. SCIAMACHY data with a SZA exceeding 87° are not considered in this comparison. SCIAMACHY stratospheric aerosol extinction values are converted to 525 nm wavelength for the comparison to SAGE II observations, using the assumed spectral dependence of the aerosol extinction coefficient. For the initial comparison of SCIAMACHY and SAGE II aerosol extinction profiles no cloud-filtering of the SCIAMACHY limb measurements was applied. The effect of clouds is later investigated using cloud occurrence information also available from SCIAMACHY. Figure 10 shows the comparison – mean profiles and relative differences ((SCIAMACHY-SAGE)/SAGE) – of the globally averaged SAGE II and SCIAMACHY stratospheric aerosol extinction profiles at 525 nm wavelength. Below 15 km, SCIAMACHY overestimates the aerosol extinction by up to 40 % as compared to SAGE II. But above 15 km the agreement is within 20 % and between 16 and 30 km even within about 10 %.

To gain more information about the meridional behavior of the retrieval, the profiles were averaged zonally and over all available co-locations as well as binned into eight 20° latitude bins between 80° N and 80° S (Fig. 11). Table 4 shows the relative differences of the retrieved aerosol extinction in comparison to co-located SAGE II measurements for the eight latitude bins. Between 20° N and 20° S values for 15 km altitude have been ignored because of tropospheric influences in these latitudes. For the same reason, the 15 km values for 20–40° N/S are put in brackets.

At low latitudes (20° N–20° S) the agreement is quite good above 20 km altitude. The relative difference is generally smaller than 20 % in both hemispheres and above the tropopause. Above 20 km altitude in the Southern Hemisphere the SCIAMACHY aerosol extinctions are up to 20 % larger than the SAGE II values. Below 20 km the frequent occurrence of tropospheric clouds makes SCIAMACHY and SAGE II products uncomparable. An analysis of the tropospheric cloud detection data set obtained with SCODA (SCIAMACHY ClOud Detection Algorithm) (Eichmann et al., 2009) showed that about 95 % of all SCIAMACHY limb measurements are affected by tropospheric clouds.

Between 20° N and 40° N, the relative differences are generally within ±20 %. Only above 30 km and below 17 km the differences are larger. In the corresponding region in the Southern Hemisphere, the shape of the relative difference profile is similar, but the values are larger than in the Northern Hemisphere, ranging from −50 % at 35 km altitude to +100 % near 15 km. However, between 20 and 30 km, the difference is generally within ±20 %. The large error below 20 km might still be an effect of tropospheric clouds.

Between 40° N and 60° N, the agreement is quite good below 25 km with relative differences to SAGE of ±20 % at most. Above 25 km, SCIAMACHY results are systematically lower than those of SAGE II, e.g. by about 50 % at 32 km. The picture of the

AMTD
5, 5993–6035, 2012

corresponding latitude bin in the Southern Hemisphere looks completely different. At all altitudes below 30 km, we see systematically higher values. At 20 km the relative difference reaches 60 %.

For latitudes between 60° and 80° we observe a significant interhemispheric difference in the relative differences between SCIAMACHY and SAGE II aerosol extinction profiles. In the Northern Hemisphere the relative differences are negative for all altitudes between 15 and 34 km (with a maximum difference of about −50 % between 25 and 30 km), whereas they are positive for all altitudes in the Southern Hemisphere remaining more or less constant at about +30 % between 15 and 30 km. In general it can be said that the SCIAMACHY retrieval results in lower stratospheric aerosol extinction in the Northern Hemisphere and higher values in the Southern Hemisphere as compared to SAGE II measurements. One possible reason for this apparent interhemispheric difference is the different sensitivity of the aerosol profile retrievals to errors in the surface albedo (see Sect. 4.2, in particular Fig. 6 panel 4). Tropospheric clouds affect the majority of the SCIAMACHY limb observations, and this will lead to a higher effective albedo at 470 nm and 750 nm as compared to the surface albedo data base by Matthews (1983) currently used by SCIATRAN for the retrieval. This is particularly true for measurements above the ocean. A low bias in the assumed albedo is most commonly associated with high bias in the aerosol extinction values, and this effect is much stronger in the Southern Hemisphere. This is qualitatively consistent with the validation results presented in Fig. 11 – particularly considering the comparisons for 40°–60° N/S and 60°–80° N/S.

This aspect was investigated further by applying the SCODA cloud detection data base (Eichmann et al., 2009) in order to exclude SCIAMACHY measurements from the comparison that were affected by clouds in the troposphere. The top panels in Fig. 12 show the relative difference between SCIAMACHY and SAGE II aerosol extinction profiles for all co-locations in the Southern Hemisphere without cloud filter applied. The bottom panels show the relative difference with all SCIAMACHY measurements removed those were affected by clouds. Unexpectedly, the cloud filtering does not improve the agreement between SCIAMACHY and SAGE II aerosol extinction, and we conclude that the overestimation of stratospheric aerosol extinction by SCIAMACHY in the Southern Hemisphere must have other reasons. A possible origin of this inter-hemispheric difference is an inappropriate aerosol phase function. This aspect will be investigated in detail in the near future.

We conclude that in a global average sense SCIAMACHY and SAGE II aerosol extinction profiles agree very well, but systematic interhemispheric differences remain that need to be investigated. Our best explanation is the selection of the phase function. Further work is now being undertaken to establish the optimal phase function for stratospheric aerosol for SCIAMACHY retrievals.

We now briefly discuss how the comparisons with SAGE II in this study compare to the results recently presented by Taha et al. (2011) and Ovigneur et al. (2011). Both of these studies also use SCIAMACHY limb measurements to infer stratospheric aerosol profiles. Taha et al. (2011) (110 co-locations with SAGE II within 250 km and 24 h) find a systematic negative bias of the SCIAMACHY aerosol extinction profiles relative to SAGE II of about 25 %.

Ovigneur et al. (2011) present comparisons with co-located SAGE II measurements for two different values of the particle mean radius (0.15 and 0.35 micron). 2000 co-locations with SAGE II have been investigated with co-location criteria of ±300 km along flight direction and ±115 km across flight direction, and a time difference of less than 12 h. In this study, the root mean square difference with respect to SAGE II is on the order of 30–50 % with a minimum of 30 % around 22 km (Ovigneur et al., 2011).

6 Sample results

Figure 13 shows the time and latitude dependence of the retrieved aerosol extinction at 525 nm for the 20 hPa (top panel) and the 70 hPa (bottom panel) pressure levels. ECMWF reanalysis data were used to interpolate the SCIAMACHY retrievals onto these pressure levels. Both panels show clear evidence for the occurrence of polar

AMTD
5, 5993–6035, 2012

stratospheric clouds during each hemispheric winter at polar latitudes. Note that even if PSCs are present the retrievals are performed with the standard assumption on the aerosol phase function, i.e. the derived extinction values are subject to potentially large systematic errors and only serve as a qualitative indicator for the presence of PSCs. The aerosol extinction at 20 hPa and at tropical latitudes shows a dominant annual cycle with a maximum during winter, i.e. around December/January in the Northern Hemisphere, and around July in the Southern Hemisphere. This annual variation is consistent with the annual variation in lidar backscatter ratio observed at Boulder (40° N) and Hawaii (19° N) (Hofmann et al., 2009). The aerosol extinction at 20 hPa also shows apparent QBO (quasi biennial oscillation) signatures – particularly pronounced in the Southern Hemisphere between 20° and 40° – that will be investigated in more detail in a forthcoming study. The 20 hPa level is too high to exhibit obvious signatures related to volcanic eruptions. At 70 hPa (bottom panel of Fig. 13) several volcanic eruptions are clearly visible, but as in the case of PSCs one should keep in mind that the assumed aerosol phase function is not representative for a volcanically enhanced stratospheric aerosol load. The effect of a volcanic stratospheric aerosol particle size distribution on the retrievals will be investigated in an upcoming study. The morphology between the eruptions of Tavurvur in October 2006 and Kasatochi in August 2008 with the minimum in the tropics in 2008 agrees very well with the evolution of the zonal mean scattering ratio at 532 nm between 17 and 21 km from CALIPSO lidar measurements shown in Fig. 1 in Solomon et al. (2011).

7 Conclusions

Stratospheric aerosol extinction profiles are retrieved from SCIAMACHY limb-scatter observations. The retrieval scheme is based on a colour-index approach combining the limb-radiance profiles at two wavelengths in the visible spectral range. The aerosols are assumed to consist of sulphate particles with a particle size distribution characteristic for background aerosol conditions. The retrieval is performed using an optimal estimation scheme driving the radiative transfer model SCIATRAN. Sensitivity studies were carried out in order to investigate the impact of uncertainties in the knowledge of several parameters (albedo, neutral density profile, O_3 profile, tangent height errors etc.) on the aerosol profile retrievals. For realistic errors in these parameters, in the Northern Hemisphere the error in the aerosol extinction was below 10 % in all cases. In the Southern Hemisphere, uncertainties in the ground albedo and in the neutral density could lead to errors in the aerosol extinction of up to 20 %.

The SCIAMACHY stratospheric aerosol extinction profile retrievals were compared to all co-located SAGE II solar occultation measurements available between August 2002 and the end of the SAGE II mission in 2005. Globally averaged the agreement between SCIAMACHY and SAGE II aerosol extinction profiles is within 20 % above 15 km altitude and even within 10 % between 16 and 30 km. However, comparisons made for specific latitude bins showed the presence of systematic interhemispheric differences, with SCIAMACHY showing lower aerosol extinction in the Southern Hemisphere and higher values in the Northern Hemisphere at mid- and high latitudes in comparison with SAGE II. We demonstrated that this interhemispheric difference is most likely not related to the interhemispheric differences in albedo sensitivity of the aerosol retrievals. The cause of this systematic difference between SAGE-II and SCIAMACHY is not yet established unambiguously. One likely candidate is the angular dependence of the phase function used in this retrieval.

Finally, first results on the global morphology of stratospheric aerosol retrieved from SCIAMACHY were presented. The retrieved aerosol extinction morphology at 70 hPa demonstrates that the retrieval scheme used is capable of identifying stratospheric signatures of volcanic eruptions.

Acknowledgements. SCIAMACHY is jointly funded by Germany, the Netherlands and Belgium. This work was in part funded by the European Space Agency (ESA), the Deutsche Zentrum für Luft- und Raumfahrt (DLR), and the University of Bremen. It provides a contribution to the following projects: ESA SPIN and SPARC data initiatives. We are also indebted to ESA for providing the SCIAMACHY Level 1 data used in this study.

References

Ackerman, M., Lippens, C., and Muller, C.: Stratospheric aerosols properties from Earth limb photography, Nature, 292, 587–591, doi:10.1038/292587a0, 1981. 5996

Bertaux, J. L., Megie, G., Widemann, T., Chassefiere, E., Pellinen, R., Kyrölä, E., Korpela, S., and Simon, P.: Monitoring of ozone trend by stellar occultations: the GOMOS instrument, Adv. Space Res., 11, 237–242, doi:10.1016/0273-1177(91)90426-K, 1991. 5996

Bourassa, A. E., Degenstein, D. A., Gattinger, R. L., and Llewellyn, E. J.: Stratospheric aerosol retrieval with optical spectograph and infrared imaging system limb scatter measurements, J. Geophys. Res., 112, D10217, doi:10.1029/2006JD008079, 2007. 5998

Bovensmann, H., Burrows, J. P., Buchwitz, M., Frerick, J., Noël, S., Rozanov, V. V., Chance, K. V., and Goede, A. P. H.: SCIAMACHY: mission objectives and measurement modes, J. Atmos. Sci., 56, 127–150, doi:10.1175/1520-0469(1999)056<0127:SMOAMM>2.0.CO;2, 1999. 5996, 5997

Brogniez, C. and Lenoble, J.: Size distribution of stratospheric aerosol from SAGE II multi-wavelength extinction, in: Aerosol and Climate, edited by: Hobbs, V. and McCormick, M., A. Deepak Pub., Hampton, Va., USA, 305–311, 1988. 5995

Brogniez, C., Santer, R., Diallo, B. S., Herman, M., Lenoble, J., and Jäger, H.: Comparative observations of stratospheric aerosols by ground-based lidar, balloon-borne polarimeter, and satellite solar occultation, J. Geophys. Res., 97, 805–823, doi:10.1029/92JD01919, 1992. 5995

Burrows, J. P., Hölzle, E., Goede, A. P. H., Visser, H., and Fricke, W.: SCIAMACHY – scanning imaging absorption spectrometer for atmospheric chartography, Acta Astronaut., 35, 445–451, doi:10.1016/0094-5765(94)00278-T, 1995. 5996, 5997

Cunnold, D. M., Gray, C. R., and Merrit, D. C.: Stratospheric aerosol layer detection, J. Geophys. Res., 78, 920–931, doi:10.1029/JC078i006p00920, 1973. 5996

Davies, C. N.: Size distribution of atmospheric particles, J. Aerosol Sci., 5, 293–300, doi:10.1016/0021-8502(74)90063-9, 1974. 6003

Deshler, T.: A review of global stratospheric aerosol: measurement, importance, life cycle, and local stratospheric aerosol, Atmos. Res., 90, 223–232, doi:10.1016/j.atmosres.2008.03.016, 2008. 5995

Eichmann, K.-U., von Savigny, C., Reichl, P., Robert, C., Steinwagner, J., Bovensmann, H., and Burrows, J. P.: SCODA: SCIAMACHY cloud detection algorithm from limb radiance measurements, Algorithm Theoretical Baseline Document (ATBD), University of Bremen, Bremen, Germany, 2009. 6009, 6010

Erle, F., Grendel, A., Perner, D., Platt, U., and Pfeilsticker, K.: Evidence of heterogeneous bromine chemistry on cold stratospheric sulphate aerosols, Geophys. Res. Lett., 25, 4329–4332, doi:10.1029/1998GL900087, 1998. 5995

Flittner, D. E., Bhartia, P. K., and Herman, B. M.: O_3 profiles retrieved from limb scatter measurements: theory, Geophys. Res. Lett., 27, 2601–2604, doi:10.1029/1999GL011343, 2000. 5999

Fussen, D. and Bingen, C.: A volcanism dependent model for the extinction profile of stratospheric aerosols in the UV-visible range, Geophys. Res. Lett., 26, 703–706, doi:10.1029/1999GL900082, 1999. 5999, 6003

Gottwald, M. and Bovensmann, H.: SCIAMACHY – Exploring the Changing Earth's Atmosphere, Springer, Dordrecht, Heidelberg, London, New York, 2011. 5998

Hanson, D. R. and Ravishankara, A. R.: Heterogeneous chemistry of bromine species in sulfuric acid under stratospheric conditions, Geophys. Res. Lett., 22, 385–388, doi:10.1029/94GL03379, 1995. 5995

Henyey, L. G. and Greenstein, J. L.: Diffuse radiation in the galaxy, Astrophys. J., 93, 70–83, doi:10.1086/144246, 1941. 6002

Hofmann, D., Barnes, J., O'Neil, M., Trudeau, M., and Neely, R.: Increase in background stratospheric aerosol observed with lidar at Mauna Loa Observatory and Boulder, Colorado, Geophys. Res. Lett., 36, L15808, doi:10.1029/2009GL039008, 2009. 6012

Hoogen, R.: Mie theory outline and IUPMIE user's guide, Internal Report, Institut für Umweltphysik, Universität Bremen, Bremen, Germany, 1995. 6002

Junge, C. E., Changnon, C. W., and Manson, J. E.: Stratospheric aerosols, J. Meteorol., 18, 81–108, doi:10.1175/1520-0469(1961)018<0081:SA>2.0.CO;2, 1961. 5995

Kauss, J.: Aerosol-Parametrisierung für Strahlungstransport-Simulationen im ultravioletten bis nahinfraroten Spektralbereich, Diploma thesis, University of Bremen, Bremen, Germany, 1998. 6002, 6003

Lee, T. F., Nelson, C. S., Dills, P., Riishojgaard, L. P., Jones, A., Li, L., Miller, S., Flynn, L. E., Jedlovec, G., McCarty, W., Hoffman, C., and McWilliams, G.: NPOESS next-generation operational global earth observations, B. Am. Meteorol. Soc., 91, 727–740, doi:10.1175/2009BAMS2953.1, 2010. 5996

Lenoble, J., Pruvost, P., and Brogniez, C.: SAGE satellite observations of stratospheric aerosols from Mount St. Helens eruption: a two wavelength analysis, J. Geophys. Res., 89, 11666–11676, doi:10.1029/JD089iD07p11666, 1984. 5995

Llewellyn, E. J., Lloyd, N. D., Degenstein, D. A., Gattinger, R. L., Petelina, S. V., Bourassa, A. E., Wiensz, J. T., Ivanov, E. V., McDade, I. C., Solheim, B. H., McConnell, J. C., Haley, C. S., von Savigny, C., Sioris, C. E., McLinden, C. A., Griffioen, E., Kaminski, J., Evans, W. F. J., Puckrin, E., Strong, K., Wehrle, V., Hum, R. H., Kendall, D. J. W., Matsushita, J., Murtagh, D. P., Brohede, S., Stegman, J., Witt, G., Barnes, G., Payne, W. F., Piche, L., Smith, K., Warshaw, G., Deslauniers, D.-L., Marchand, P., Richardson, E. H., King, R. A., Wevers, I., McCreath, W., Kyrölä, E., Oikarinen, L., Leppelmeier, G. W., Auvinen, H., Megie, G., Hauchecorne, A., Lefevre, F., de La Noe, J., Ricaud, P., Frisk, U., Sjoberg, F., von Scheele, F., and Nordh, L.: The OSIRIS instrument on the Odin spacecraft, Can. J. Phys., 82, 411–422, doi:10.1139/P04-005, 2004. 5996

Lumpe, J. D., Bevilacqua, R. M., Hoppel, K. W., Krigman, S. S., Kriebel, D. L., Randall, C. E., Rusch, D. W., Brogniez, C., Ramananaherosa, R., Shettle, E. P., Olivero, J. J., Lenoble, J., and Pruvost, P.: POAM II retrieval algorithm and error analysis, J. Geophys. Res., 102, 23593–23614, doi:10.1029/2002JD002137, 1997. 5995

Matthews, E.: Global vegetation and land use: new high resolution data base for climate studies, J. Clim. Appl. Meteorol., 22, 474–487, doi:10.1175/1520-0450(1983)022<0474:GVALUN>2.0.CO;2, 1983. 6008, 6010

McCormick, M. P. and Trepte, C. R.: SAM II measurements of Antarctic PSC's and aerosols, Geophys. Res. Lett., 13, 1276–1279, doi:10.1029/GL013i012p01276, 1986. 5995

McCormick, M. P. and Veiga, R. E.: SAGE II measurements of early Pinatubo aerosols, Geophys. Res. Lett., 19, 155–158, doi:10.1029/91GL02790, 1992. 5995

McLinden, C. A., McConnell, J. C., McElroy, C. T., and Griffioen, E.: Observations of stratospheric aerosol using CPFM polarized limb radiances, J. Atmos. Sci., 56, 233–240, doi:10.1175/1520-0469(1999)056<0233:OOSAUC>2.0.CO;2, 1999. 5996

Ovigneur, B., Landgraf, J., Snel, R., and Aben, I.: Retrieval of stratospheric aerosol density profiles from SCIAMACHY limb radiance measurements in the O_2 A-band, Atmos. Meas. Tech., 4, 2359–2373, doi:10.5194/amt-4-2359-2011, 2011. 5997, 6011

Randel, W., Wu, F., and Gaffen, D.: Interannual variability of the tropical tropopause derived from radiosonde data and NCEP reanalyses, J. Geophys. Res., 105, 15509–15523, doi:10.1029/2000JD900155, 2000. 6003

Rodgers, C. D.: Inverse Methods for Atmospheric Sounding: Theory and Practice, World Scientific, Singapore, 2000. 6001

Rosen, J. M.: The boiling point of stratospheric aerosols, J. Appl. Meteorol., 10, 1044–1046, doi:10.1175/1520-0450(1971)010<1044:TBPOSA>2.0.CO;2, 1971. 5995

Rozanov, A., Rozanov, V., Buchwitz, M., Kokhanovsky, A., and Burrows, J. P.: SCIATRAN 2.0 – a new radiative transfer model for geophysical applications in the 175–2400 nm spectral region, Adv. Space Res., 36, 1015–1019, doi:10.1016/j.asr.2005.03.012, 2005. 6001, 6002

Self, S., Zhao, J.-X., Holasek, R. E., Torres, R. C., and King, A. J.: The atmospheric impact of the 1991 Mount Pinatubo eruption, in: Fire and Mud: Eruptions and Lahars of Mount Pinatubo, Philippines, edited by: Newhall, C. G. and Punongbayan, R. S., University of Washington Press, Washington, 1997. 5994

Solomon, S., Sanders, R. W., Garcia, R. R., and Keys, J. G.: Increased chlorine dioxide over Antarctica caused by volcanic aerosols from Mount Pinatubo, Nature, 363, 245–248, doi:10.1038/363245a0, 1993. 5995

Solomon, S., Daniel, J. S., Neely III, R. R., Vernier, J.-P., Dutton, E. G., and Thomason, L. W.: The persistently variable "background" stratospheric aerosol layer and global climate change, Science, 333, 866–870, doi:10.1126/science.1206027, 2011. 6012

Taha, G., Rault, D. F., Loughman, R. P., Bourassa, A. E., and von Savigny, C.: SCIAMACHY stratospheric aerosol extinction profile retrieval using the OMPS/LP algorithm, Atmos. Meas. Tech., 4, 547–556, doi:10.5194/amt-4-547-2011, 2011. 5997, 6011

Thomason, L. W.: A diagnostic stratospheric aerosol size distribution inferred from SAGE II measurements, J. Geophys. Res., 96, 22501–22508, doi:10.1029/91JD02521, 1991. 6008

Thomason, L. W., Peter, T., Carslaw, K. S., Kärcher, B., Notholt, J., Bingemer, H., Hamill, P., Brogniez, C., Deshler, T., Anderson-Sprecher, R., Weisenstein, D., and Bekki, S.: SPARC Assessment of Stratospheric Aerosol Particles, World Climate Research Programme (WCRP) SPARC Project Report 4, 1–320, 2006. 6003 von Savigny, C., Haley, C. S., Sioris, C. E., McDade, I. C., Llewellyn, E. J., Degenstein, D., Evans, W. F. J., Gattinger, R. L., Griffioen, E., Kyrölä, E., Lloyd, N. D., McConnell, J. C., McLinden, C. A., Mégie, G., Murtagh, D. P., Solheim, B., and Strong, K.: Stratospheric ozone profiles retrieved from limb scattered sunlight radiance spectra measured by the OSIRIS instrument on the Odin satellite, Geophys. Res. Lett., 30, 1755, doi:10.1029/2002GL016401, 2003. 5999

von Savigny, C., Kaiser, J. W., Bovensmann, H., Burrows, J. P., McDermid, I. S., and Leblanc, T.: Spatial and temporal characterization of SCIAMACHY limb pointing errors during the first three years of the mission, Atmos. Chem. Phys., 5, 2593–2602, doi:10.5194/acp-5-2593-2005, 2005. 6007

von Savigny, C., Bovensmann, H., Bramstedt, K., Dikty, S., Ebojie, F., Jones, A., Noël, S., Rozanov, A., and Sinnhuber, B.-M.: Indications for long-term trends and seasonal variations in the SCIAMACHY Level 1 version 6.03 tangent height information, SCIAMACHY Technical Note, TN-IUP-scia-pointing-2009-01, University of Bremen, Bremen, Germany, 2009. 6007

Wiscombe, W. J.: Improved Mie scattering algorithms, Appl. Opt., 19, 1505–1509, doi:10.1364/AO.19.001505, 1980. 6002

AMTD

5, 5993–6035, 2012

Stratospheric aerosol profiles from SCIAMACHY

F. Ernst et al.

Table 1. Typical SCIAMACHY solar zenith angle (SZA) and solar azimuth angle (SAA) at the tangent point for 5 latitudes on 21 September.

Latitude	SZA	SAA
83° N	84°	38°
40° N	48°	60°
0°	36°	105°
40° S	58°	145°
75° S	88°	155°

AMTD
5, 5993–6035, 2012

Table 2. Relative error (%) of the aerosol extintion due to uncertainties in ground albedo (uncertainty 0.15) and neutral density (3 %) for the SCIAMACHY viewing geometry at 83° N, 40° N, 0°, 40° S, and 75° S.

Alt. (km)	83° N		40° N		0°		40° S		75° S	
	Alb.	Dens.	Alb.	Dens.	Alb.	Dens.	Alb.	Dens.	Alb.	Dens.
15	< 1	5	1	8	5	10	8	12	1	20
20	< 1	2	2	1	7	2	12	3	3	15
25	< 1	0	2	1	8	2	15	1	3	5
30	< 1	2	2	2	8	2	15	0	4	5
35	< 1	2	3	2	8	3	15	2	5	5
Mean	< 1	2	2	4	7	5	12	5	3	10

AMTD
5, 5993–6035, 2012

Table 3. Relative error (%) of the aerosol extintion due to uncertainties in the ozone profile (15 %) and tangent height (200 m) for the SCIAMACHY viewing geometry at 83° N and 0° and 40° N, respectively.

Alt. (km)	O_3		TH
	83° N	0°	40° N
15	2	1	8
20	2	1	2
25	1	0.5	3
30	0	0.5	5
35	0	0.5	3
Mean	1	1	4

AMTD
5, 5993–6035, 2012

Table 4. Relative difference (%) of the SCIAMACHY aerosol extinction in comparison to co-located SAGE II measurements, both averaged in 8 latitude bins.

Alt. (km)	60–80° N	40–60° N	20–40° N	0–20° N	0–20° S	20–40° S	40–60° S	60–80° S
15	0	10	(30)	–	–	(> 100)	50	35
20	−20	5	10	−10	5	40	60	35
25	−45	−15	0	5	20	15	35	25
30	−35	−35	−5	0	10	−5	5	25
Mean	−25	−10	0	0	10	15	40	30

AMTD
5, 5993–6035, 2012

Stratospheric aerosol profiles from SCIAMACHY

F. Ernst et al.

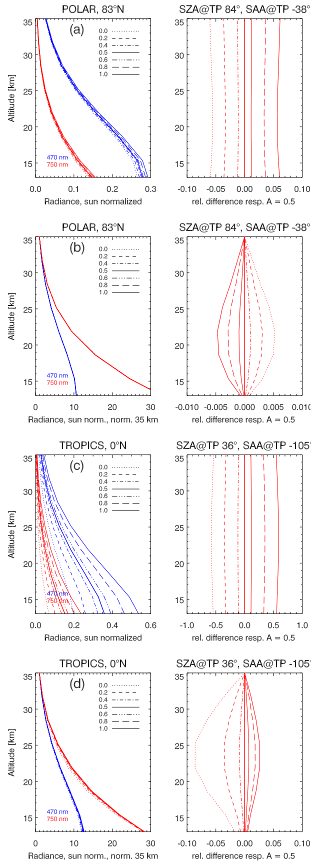

Fig. 1. Effect of the tangent height normalization: simulated radiance for $\lambda = 470$ nm (blue) and $\lambda = 750$ nm (red) with 7 different ground albedos. Top 2 panels: polar geometry (83° N) without **(a)** and with **(b)** tangent height normalization; bottom 2 panels: tropical geometry (0°) without **(c)** and with **(d)** tangent height normalization. Relative deviations with respect to an albedo of 0.5 for $\lambda = 750$ nm are shown on the right.

AMTD
5, 5993–6035, 2012

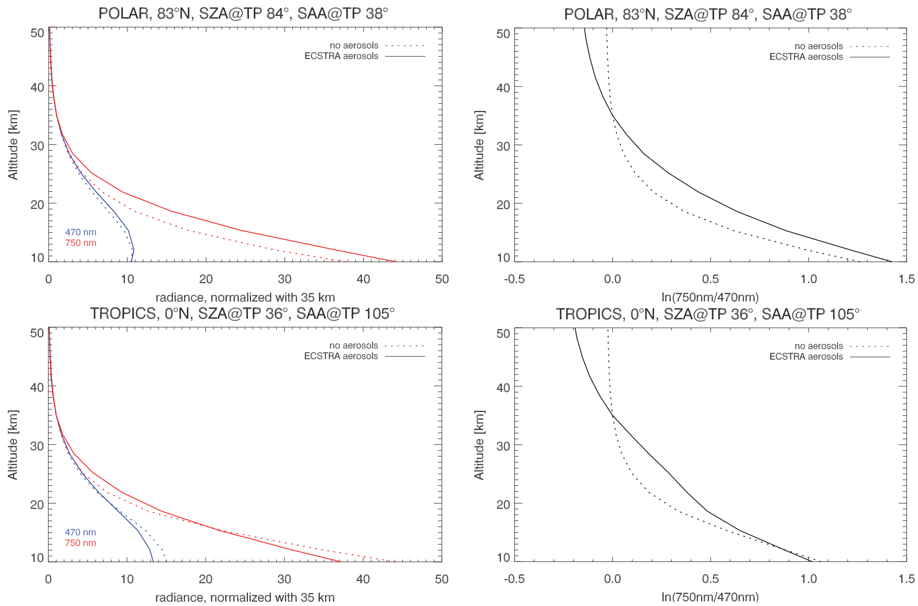

Fig. 2. Effect of the color-index-ratio: simulated tangent height normalized radiance with ground albedo $A = 0.3$ for $\lambda_s = 470$ nm and $\lambda_l = 750$ nm (left panels) and the logarithm of the ratio of both (right panels). Top panels: polar geometry (83° N), bottom panels: tropical geometry (0°).

AMTD
5, 5993–6035, 2012

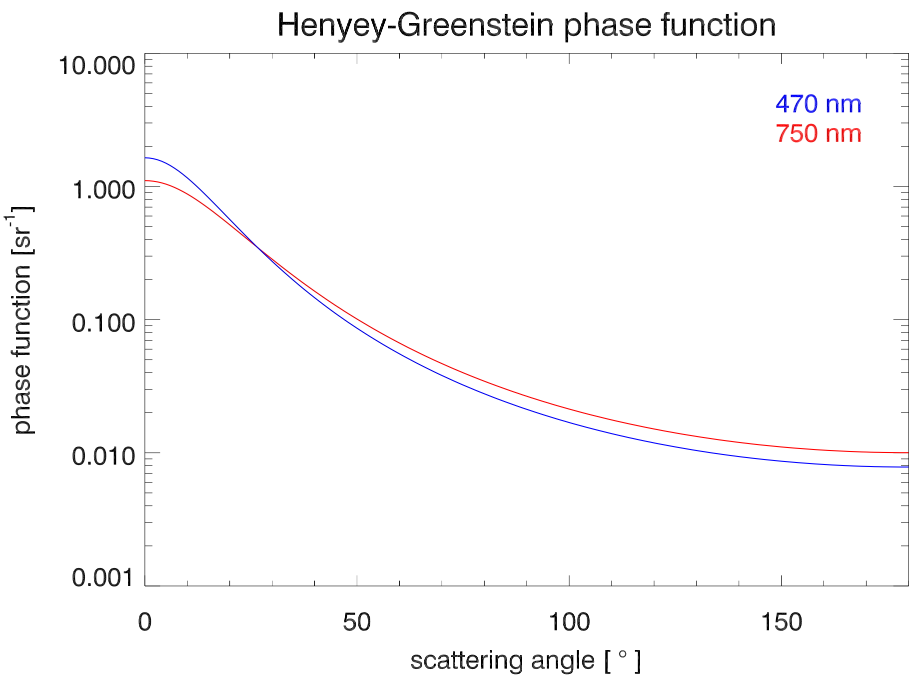

Fig. 3. Henyey-Greenstein phase function for the 2 wavelengths used in this paper. The asymmetry parameters for stratospheric aerosols are $g(470\,\mathrm{nm}) = 0.712$, $g(750\,\mathrm{nm}) = 0.655$.

AMTD
5, 5993–6035, 2012

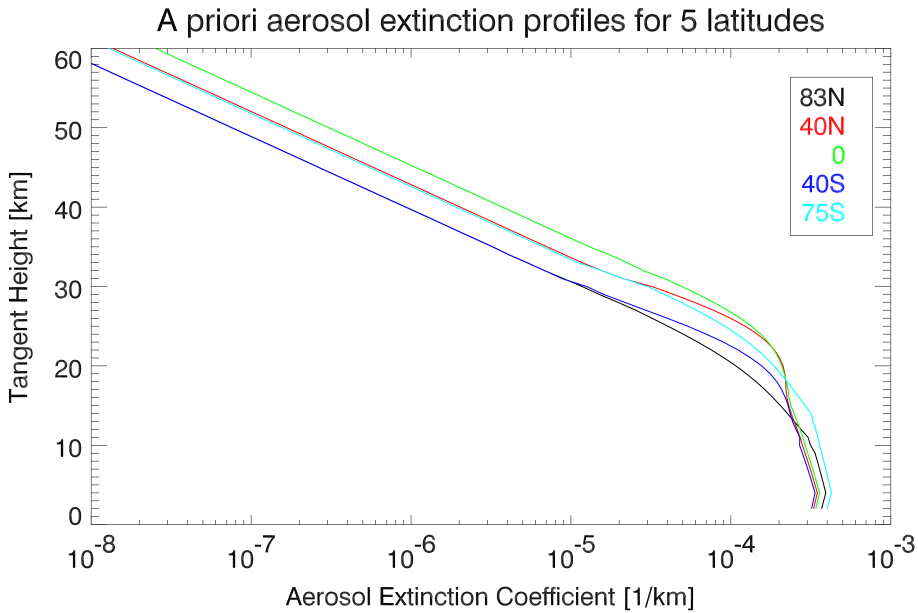

Fig. 4. The modified a priori aerosol extinction profiles for the 5 latitudes 83° N, 40° N, 0°, 40° S, and 75° S.

AMTD
5, 5993–6035, 2012

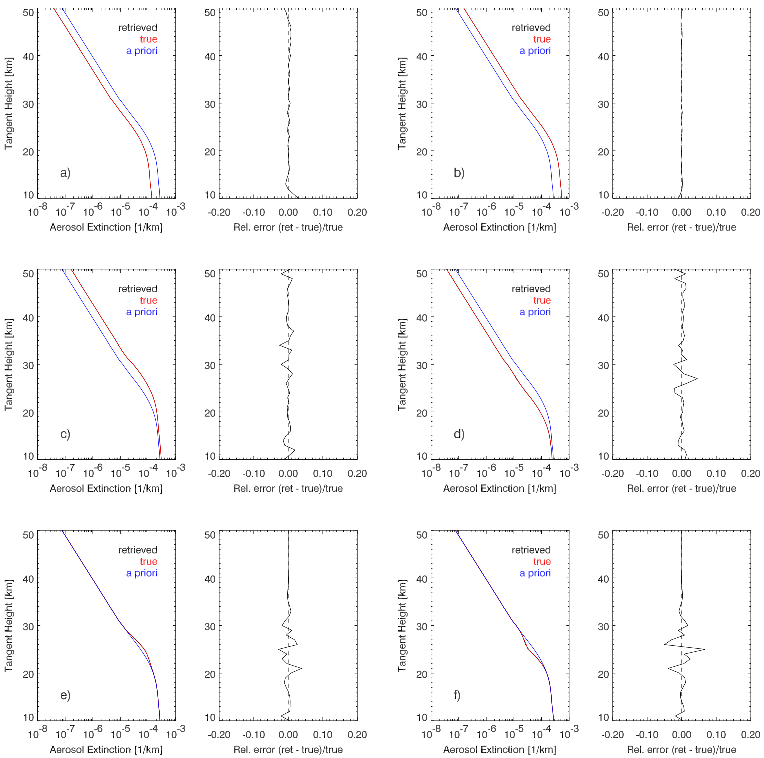

Fig. 5. Synthetic retrievals with the 6 modifications. Left panels: True and a priori aerosol extinction profiles. Right panels: relative difference between the true and the retrieved aerosol extinction profiles. Modifications of the "true" profile in comparison to the a priori profile: **(a)** multiplied by 0.5; **(b)** multiplied by 2; **(c)** altitude shift +3 km; **(d)** altitude shift −3 km; **(e)** artificial maximum around 25 km; **(f)** artificial minimum around 25 km.

AMTD
5, 5993–6035, 2012

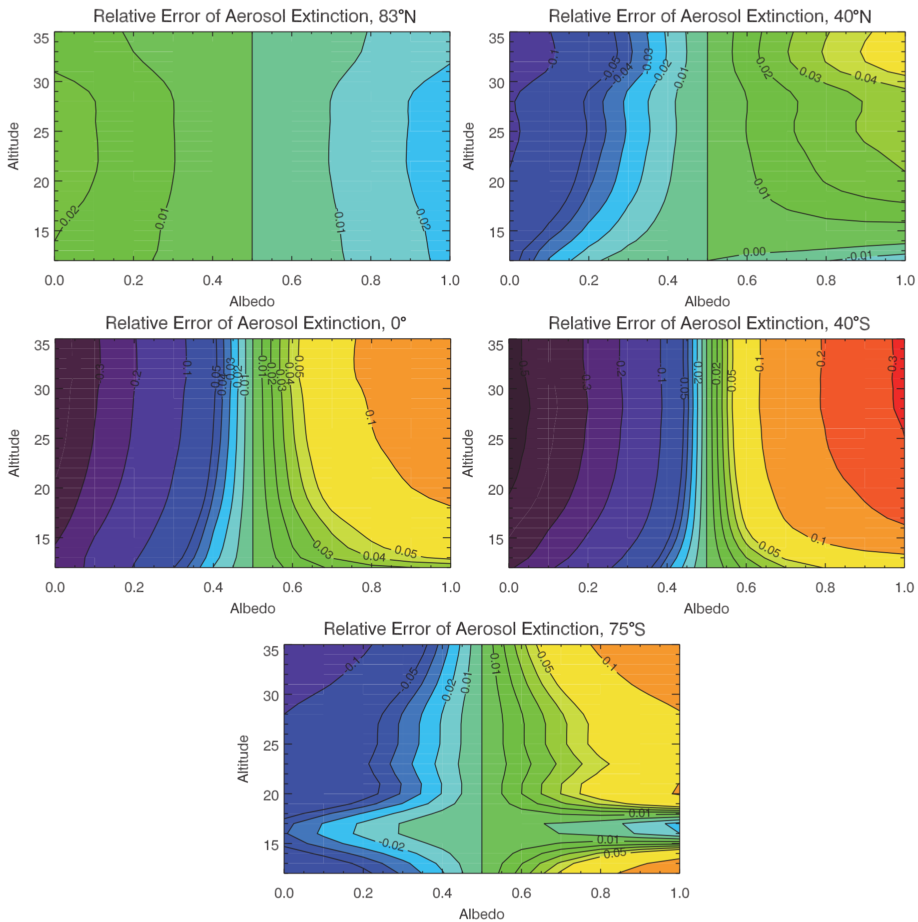

Fig. 6. Relative errors in the retrieved aerosol extinction coefficients for different values of the true surface albedo A and the SCIAMACHY viewing geometry at 83° N, 40° N, 0°, 40° S, and 75° S. The albedo assumed for the retrieval is $A = 0.5$.

AMTD
5, 5993–6035, 2012

Stratospheric aerosol profiles from SCIAMACHY

F. Ernst et al.

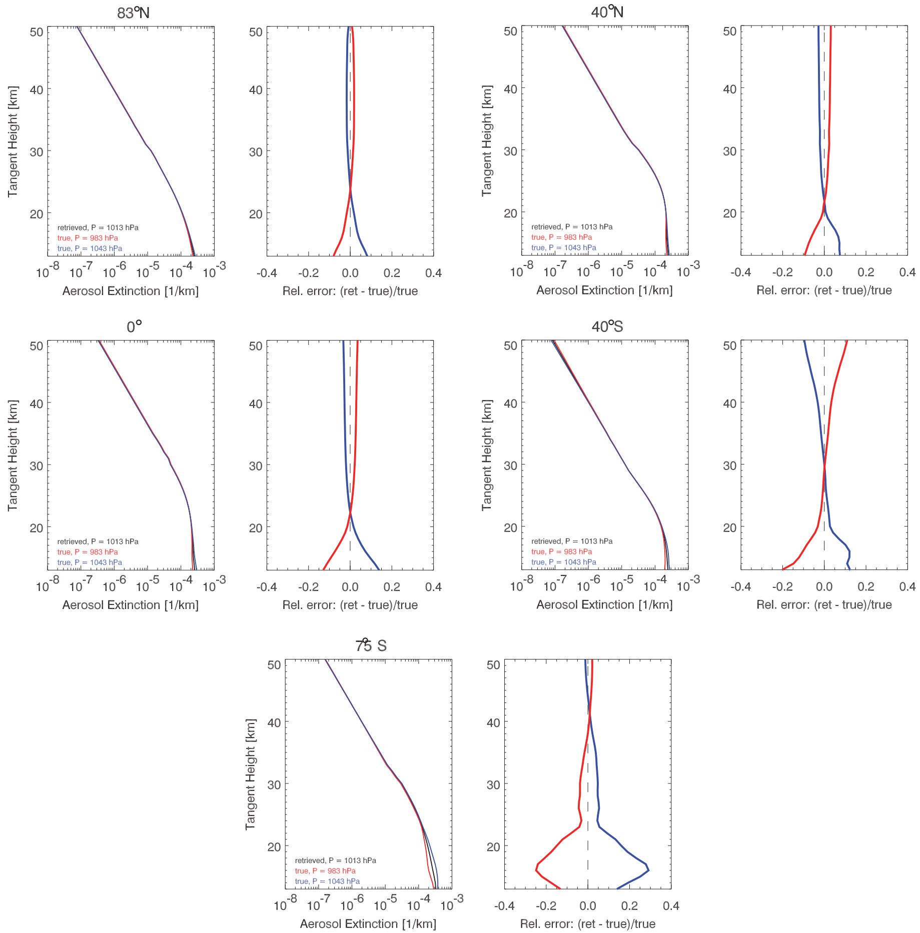

Fig. 7. Relative aerosol extinction retrieval error for an error of about ±3 % in the neutral density and the SCIAMACHY viewing geometry at 83° N, 40° N, 0°, 40° S, and 75° S.

AMTD
5, 5993–6035, 2012

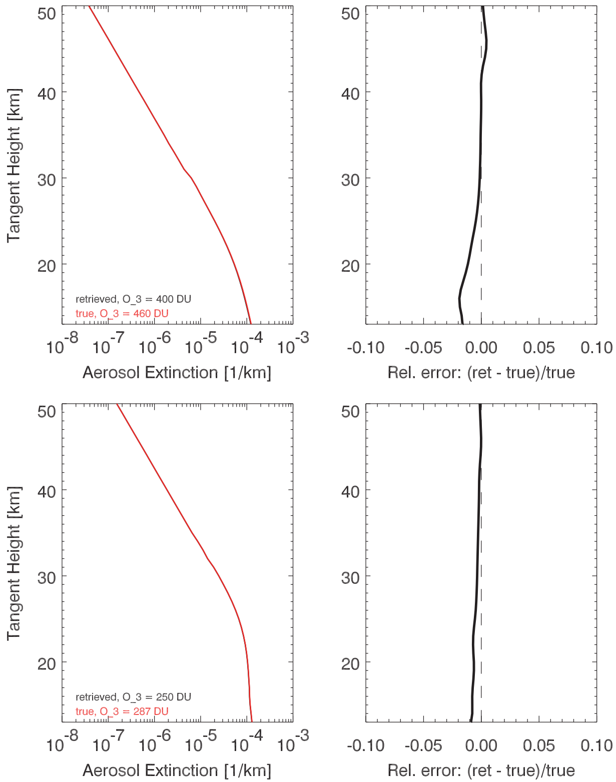

Fig. 8. Relative error in the retrieved aerosol extinction coefficient for an error of +15 % in the ozone profile for a polar and a tropical SCIAMACHY viewing geometry. Top panel: 83° N, 400 DU + 15 %; bottom panel: 0°, 250 DU + 15 %.

AMTD
5, 5993–6035, 2012

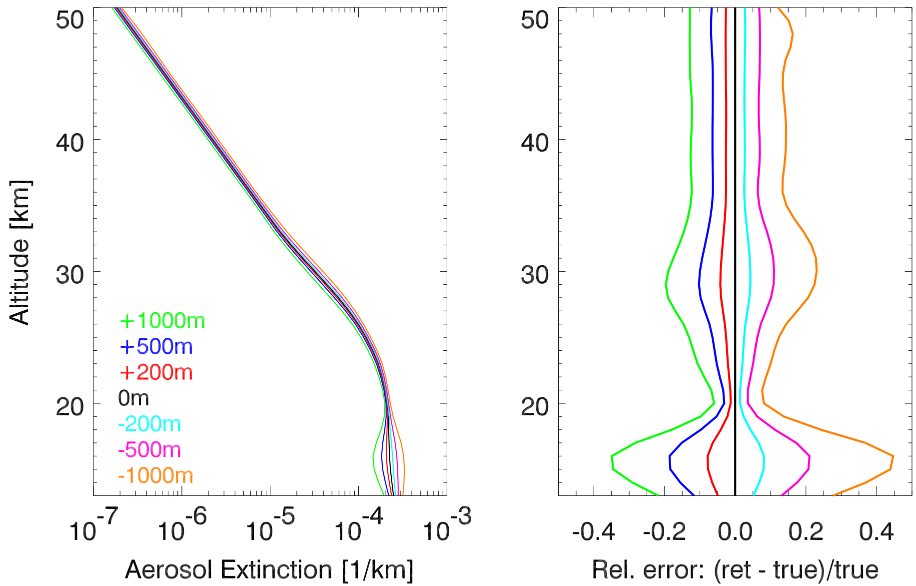

Fig. 9. Relative error in the retrieved aerosol extinction coefficient for a tangent height error of ±200 m, ±500 m, and ±1000 m for a northern mid-latitude SCIAMACHY viewing geometry.

AMTD
5, 5993–6035, 2012

Stratospheric aerosol profiles from SCIAMACHY

F. Ernst et al.

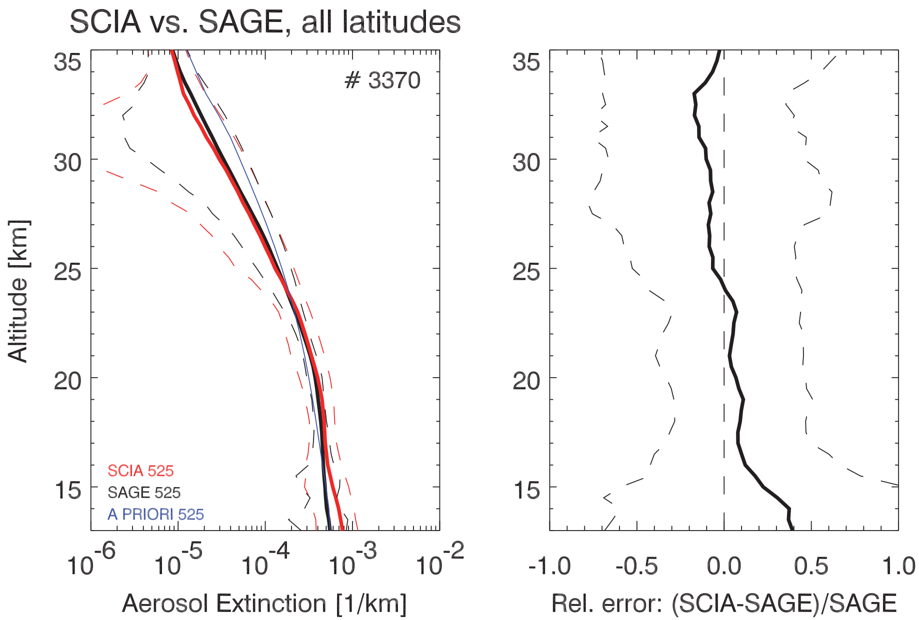

Fig. 10. Left panel: comparison of average co-located SAGE II (black) and SCIAMACHY (red) aerosol extinction profiles with standard deviation (dashed lines). The blue line shows the a priori extinction profile used for the SCIAMACHY retrievals. The number in the top right corner shows the number of co-locations averaged. Right panel: mean relative difference between SCIAMACHY and SAGE II aerosol extinction profiles with standard deviation (dashed).

AMTD
5, 5993–6035, 2012

Stratospheric aerosol profiles from SCIAMACHY

F. Ernst et al.

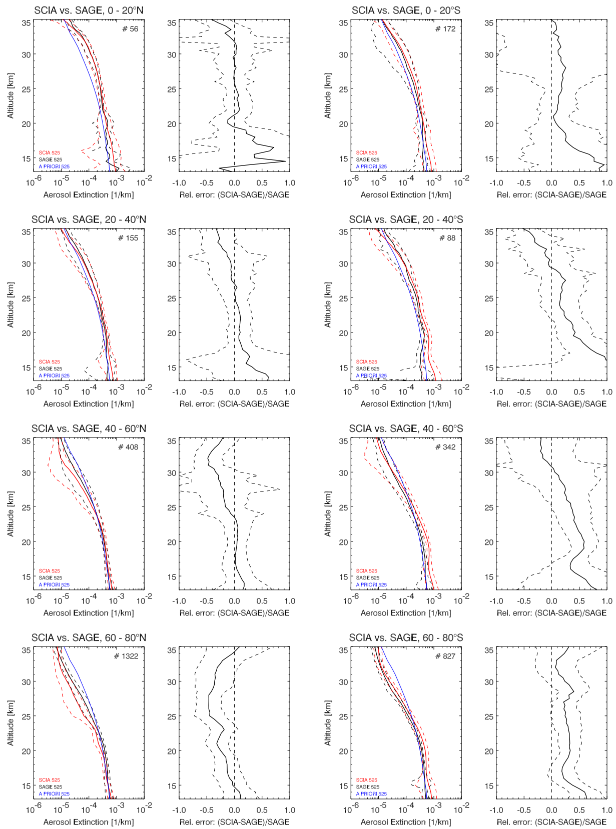

Fig. 11. Left panels: comparison of the retrieved 525 nm aerosol extinction profiles (red) with SAGE II aerosol extinction (black) and a priori profile (blue) in 8 latitude bins with standard deviation (dashed lines). Right panels: mean relative difference between SCIAMACHY and SAGE II aerosol extinction profiles with standard deviation (dashed).

AMTD

5, 5993–6035, 2012

Stratospheric aerosol profiles from SCIAMACHY

F. Ernst et al.

Title Page
Abstract | Introduction
Conclusions | References
Tables | Figures
◀| |▶
◀ ▶
Back | Close
Full Screen / Esc
Printer-friendly Version
Interactive Discussion

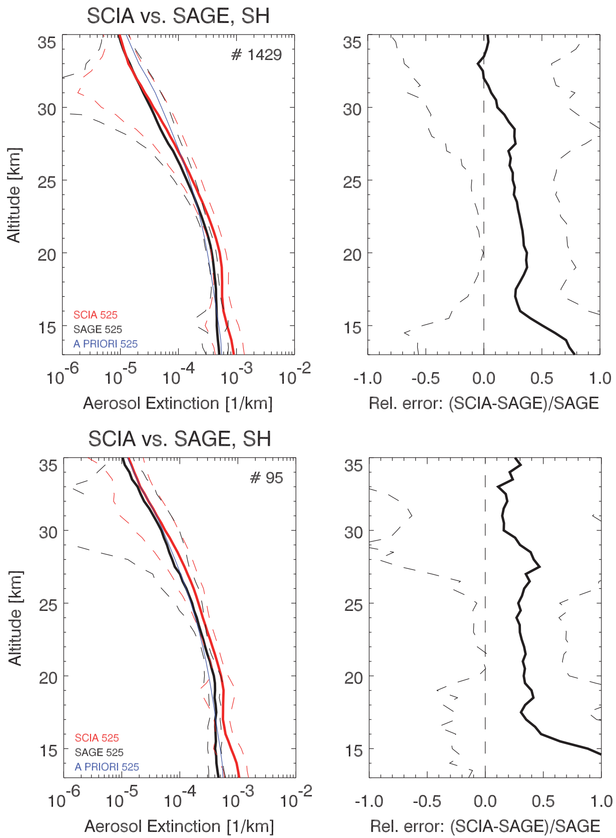

Fig. 12. Comparison of SCIAMACHY and SAGE II aerosol extinction profiles at 525 nm wavelength for Southern Hemisphere co-locations only. Top panel: no cloud screening applied. Bottom panel: only SCIAMACHY observations not affected by tropospheric clouds are used.

AMTD
5, 5993–6035, 2012

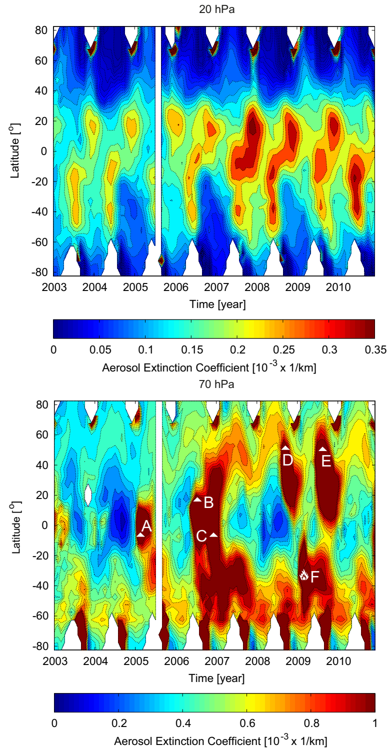

Fig. 13. Temporal and latitude variation of stratospheric aerosol extinction at 20 hPa (top panel, approx. 27 km altitude) and 70 hPa (bottom panel, approx. 18 km altitude) retrieved from SCIAMACHY limb scatter observations. Volcanic eruptions indicated by strong stratospheric aerosol extinction signals at 70 hPa level: (A) Manam (January 2005, 4° S); (B) Soufriere Hills (May 2006, 16° N); (C) Tavurvur (October 2006, 4° S); (D) Kasatochi (August 2008, 52° N); (E) Sarychev Peak (June 2009, 48° N). (F) indicates the Australian bush fires in February 2009 at 38° S.

AMTD
5, 5993–6035, 2012

Stratospheric aerosol profiles from SCIAMACHY

F. Ernst et al.